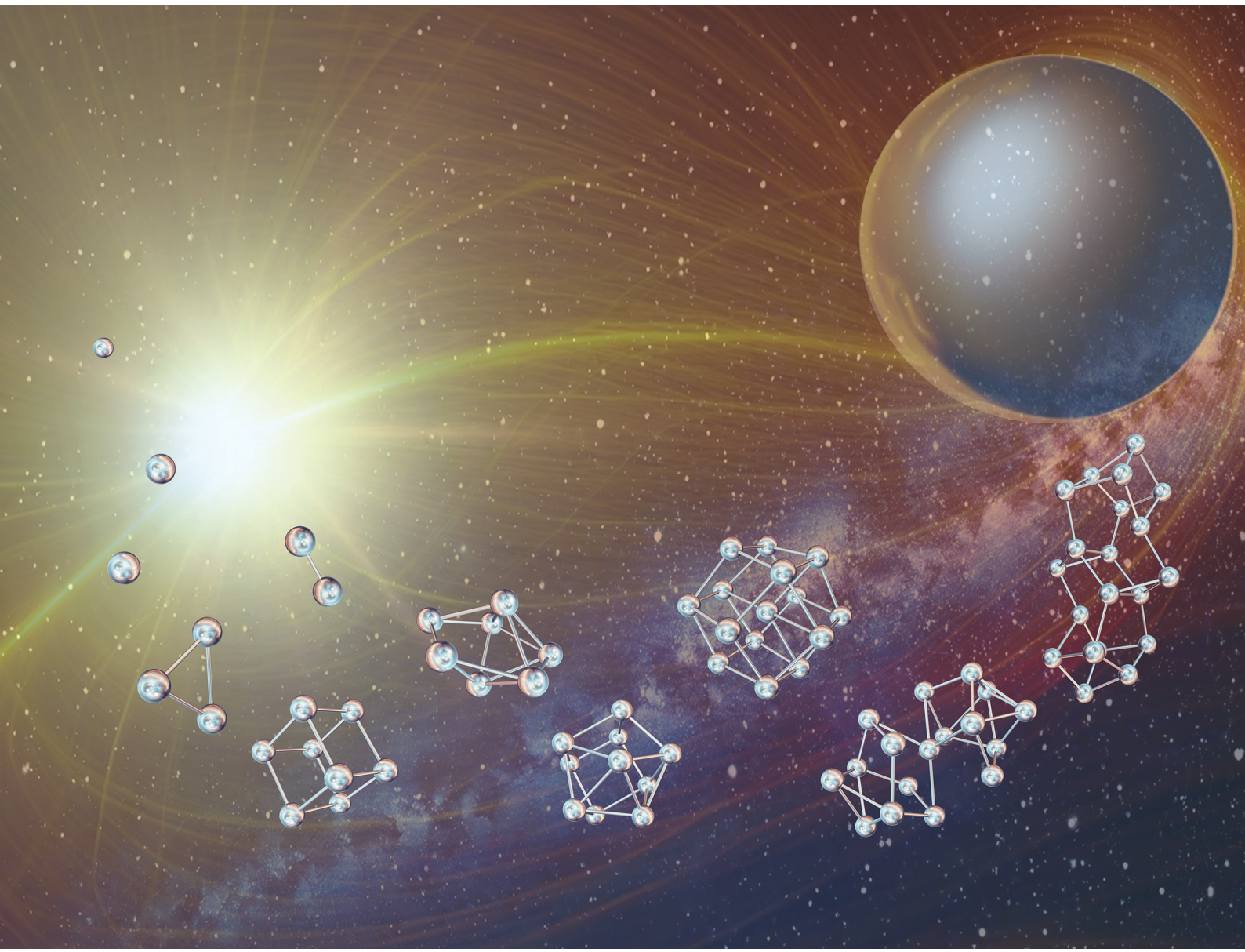


# Dalton Transactions

An international journal of inorganic chemistry

[rsc.li/dalton](http://rsc.li/dalton)



ISSN 1477-9226



Cite this: *Dalton Trans.*, 2024, **53**, 17429

Received 20th June 2024,  
Accepted 28th August 2024  
DOI: 10.1039/d4dt01797h  
[rsc.li/dalton](http://rsc.li/dalton)

## Overview and perspectives on metalloid tin cluster chemistry

R. Kimmich and A. Schnepf  \*

Although the first metalloid tin cluster was discovered by Wiberg in 1999, the number of isolated and characterized compounds is still low. However, numerous theoretical calculations indicate that a large variety of compounds are yet to be discovered, thereby suggesting that larger clusters might form a cluster-of-clusters arrangement rather than compact structures. This trend seems to be supported by the largest metalloid tin clusters exhibiting up to 20 tin atoms. In this review, recent results and future possibilities of this fascinating class of metalloid tin cluster compounds are discussed.

## Introduction

The investigation of subvalent compounds of the heavier group 14 element tin is ongoing for a considerable period of time owing to the fascinating properties of these compounds. In the 1990s, Sita and co-workers discovered [1.1.1]propellanes with unusual bonding features, which exhibit tin(0) atoms capped by stannylenes units.<sup>1–3</sup> Additionally, they were able to synthesize interesting new cluster compounds using tin precursors as building blocks for more complex molecules *via* a wide range of reactions.<sup>4–6</sup> In the following years, metal clusters

gained more popularity, and the interest in the synthesis and characterization of metal-rich compounds increased. Through the input of Schnöckel and co-workers, metalloid clusters, especially those of group 13 elements aluminium and gallium, became a fruitful field of research to gain insights into the fundamental processes of the formation and dissolution of metals from/to molecular compounds.<sup>7</sup> Thus, metal-rich metalloid clusters can be seen as ideal model compounds for this molecular area and are often stabilized by bulky ligands, partly exhibiting structural motives already known from the solid-state structure of the metal itself. Hence, these clusters are perfect, atomically precise model compounds for metal nanoparticles. In the field of metalloid tin clusters, the number of compounds is still quite low to date. Nevertheless, theoretical calculations

Chemistry Department, University of Tübingen, Auf der Morgenstelle 18, 72076 Tübingen, Germany. E-mail: [andreas.schnepf@uni-tuebingen.de](mailto:andreas.schnepf@uni-tuebingen.de)



R. Kimmich

preparing his PhD thesis on the preparation and investigation of subvalent tin and cluster compounds.



A. Schnepf

Materials at the University of Tübingen. His research interest is focused on the synthesis and application of metalloid group 14 and group 11 clusters to enlighten the nanoscale area between molecules and the bulk phase on an atomic scale.



and recent experimental results indicate that during the formation of larger clusters or nanoparticles with dozens to hundreds of tin atoms in the cluster core, an area is realized where these larger cluster compounds can be described as an agglomeration of smaller cluster units and might be described as a cluster of clusters.<sup>8,9</sup> Thus, the calculations indicate that compact structures become favourable only at a very large cluster size of about 309 tin atoms. Hence, in the case of smaller clusters, a cluster-of-clusters arrangement with principal  $\text{Sn}_{15}$  units is energetically favourable. These calculations are supported by gas phase investigations, where naked tin clusters with up to 25 tin atoms might also be described as cluster of clusters with principal  $\text{Sn}_9$  and  $\text{Sn}_{10}$  units.<sup>8</sup> This cluster-of-clusters growth pattern seems to be valid up to a certain size of nanoparticles, as observed by Uhlig and co-workers. They observed that spherical nanoparticles are composed of smaller spheres and thus might be seen as particle of particles.<sup>10</sup> In the following sections, we will provide an overview of the chemistry of metalloid tin clusters and highlight their potential use as ligands or building blocks to generate larger and more complex structures.

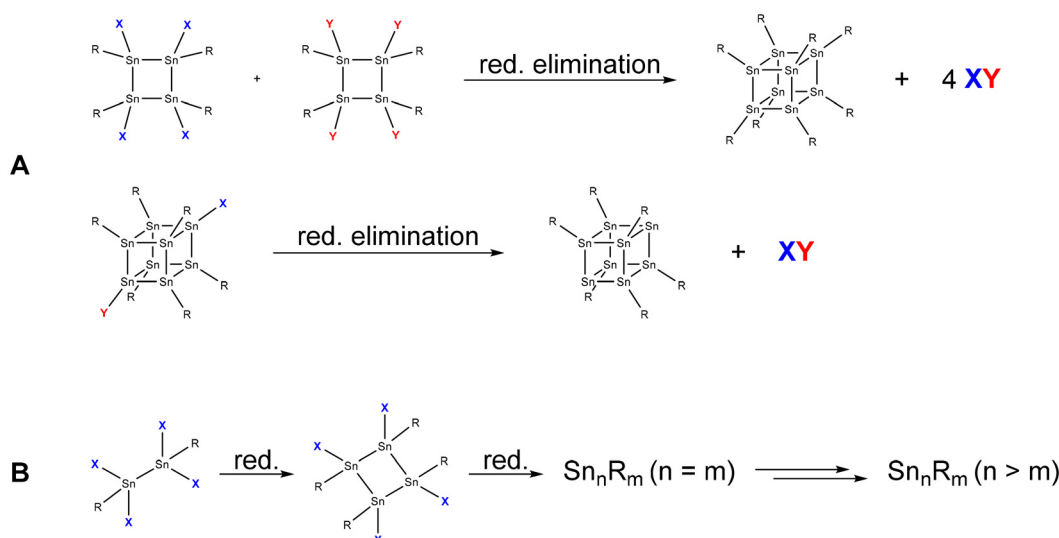
## Synthesis *via* reductive coupling

The most straightforward synthesis strategy for the formation of metalloid tin cluster compounds is *via* the reductive coupling or reductive elimination of tin-containing precursors (Scheme 1). Thereby, even metalloid clusters might be obtained if the complete elimination of substituents takes place during the reduction.

Following this synthetic approach, Wiberg and co-workers were able to synthesize the first metalloid tin cluster  $[\text{Sn}_8(\text{Si}^t\text{Bu}_3)_6]^{2-}$  **1** in 1999 (Fig. 1).<sup>11</sup> Wiberg's  $[\text{Sn}_8(\text{Si}^t\text{Bu}_3)_6]^{2-}$  cluster shows a nearly perfect cubic arrangement of the eight tin atoms with minimal distortion (Sn-Sn-Sn angles from 88.06(3)

to 91.62(3) $^\circ$ ). Hence, the bonding of an  $\text{SnR}$  or  $\text{Sn}^-$  unit seems to be similar, also showing the relation to the fully saturated clusters  $\text{Sn}_8\text{R}_8$  ( $\text{R} = \text{Si}^t\text{Bu}_2\text{Me}^{12}$  or 2,6-diethylphenyl<sup>6</sup>), which also show a cubic arrangement of the eight tin atoms.

However, the cubic arrangement of eight group 14 atoms within a group 14  $\text{E}_8\text{R}_x$  cluster depends on the number and kind of substituents present. This is directly obvious within the metalloid  $\text{Ge}_8\text{R}_6$  clusters ( $\text{R} = \text{N}(\text{SiMe}_3)_2$ ;<sup>13</sup> 2,6-( $\text{BuO}$ )<sub>2</sub>- $\text{C}_6\text{H}_3$ <sup>14</sup>), which show a distorted or an ideal cubic arrangement depending on the kind of ligand used. Also, the number of substituents plays a crucial role, as shown by Power and co-workers for the metalloid  $\text{Sn}_8\text{R}_4$  cluster **2** ( $\text{R} = 2,6\text{-Me}_2\text{C}_6\text{H}_3$ ; Mes = 2,4,6-Me<sub>3</sub>C<sub>6</sub>H<sub>2</sub>), in which the cubic  $\text{Sn}_8$  core is strongly distorted (Sn-Sn-Sn angles range from 56.24(4) to 112.38(5) $^\circ$ ).<sup>15</sup> This distortion might be due to the substitution pattern and the high steric demand of the substituents. Nevertheless, the naked tin atoms in **2** are still available for subsequent reactions, thereby leading to the decomposition of the cluster. Hence, the reaction of **2** with hydrogen gives the saturated four-membered ring compound  $(\text{SnHR})_4$  and elemental tin. This first example already shows that such metalloid cluster compounds can react with small molecules, thereby also giving an insight into heterogeneous catalytic processes.<sup>16</sup> In the subsequent years, only a few additional examples of metalloid tin clusters obtained *via* reductive coupling have been reported. In 2016, the group of Schulz and co-workers synthesized  $\text{Sn}_{10}(\text{trip})_8$ <sup>17</sup> **3** (trip = 2,4,6- $\text{i}\text{Pr}_3\text{C}_6\text{H}_2$ ) while Power and co-workers synthesized the  $\text{Sn}_{15}\text{R}_6$  **4** ( $\text{R} = \text{N}(2,6\text{-}\text{i}\text{Pr}_2\text{C}_6\text{H}_3)(\text{SiMe}_2\text{Ph})$ ), which exhibits a body-centred, cubic-like arrangement of the tin atoms in the cluster core. This arrangement is realized for tin only in a high-pressure modification above  $45 \pm 5$  GPa.<sup>18</sup> As **4** is synthesized at normal pressure and room temperature, this shows that within the metalloid clusters, arrangements can be realized that are obtained for the element only at high pressure. Similar results are also observed within metalloid gallium<sup>19</sup> or germanium<sup>20</sup> clusters. The largest metalloid tin



**Scheme 1** Exemplary formation of tin cluster compounds *via* reductive elimination (A) and reductive coupling (B).



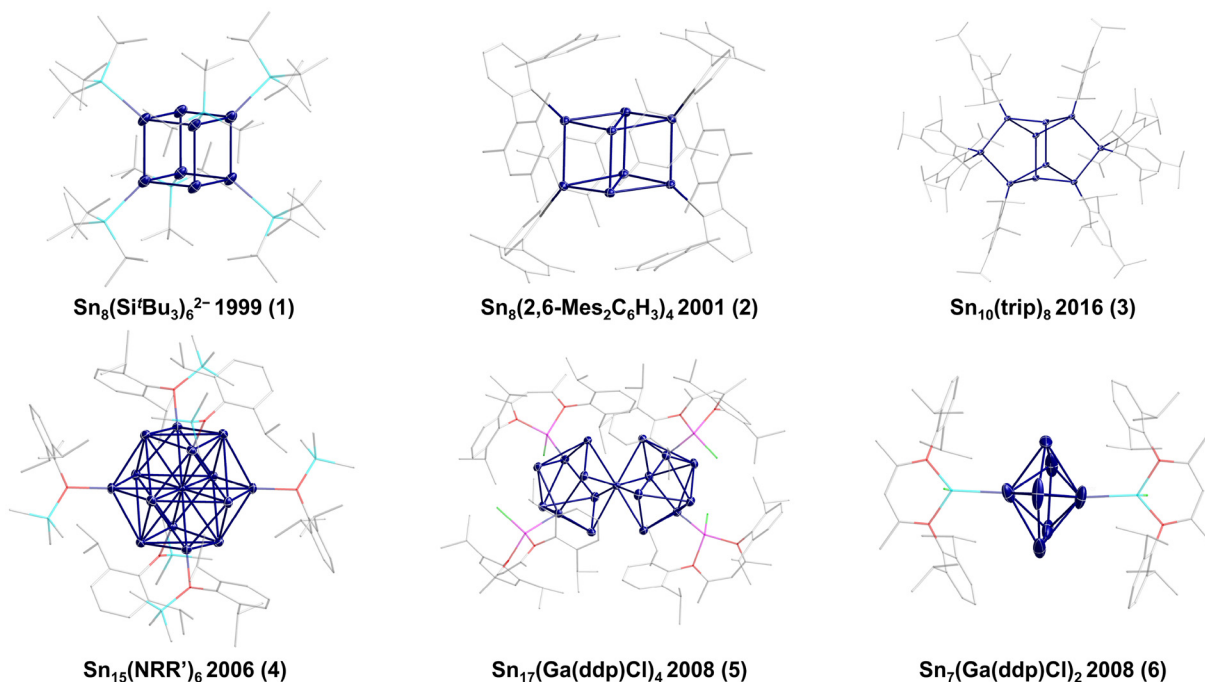


**Fig. 1** Overview of metalloid tin clusters synthesized *via* a reductive approach. Ligands are simplified by wires and sticks (light blue = silicon, light grey = carbon, violet = gallium, green = chlorine, and dark blue = tin).

cluster *via* reductive coupling was presented by Fischer and co-workers, who were able to synthesize a Sn<sub>17</sub> cluster Sn<sub>17</sub>R<sub>4</sub> 5 (R = Ga(ddp)Cl; ddp = HC(CMeNC<sub>6</sub>H<sub>3</sub>-2,6-<sup>i</sup>Pr<sub>2</sub>)<sub>2</sub>), which is crystallized together with the metalloid cluster Sn<sub>7</sub>R<sub>2</sub> 6, bearing the same substituent.<sup>21</sup> The Sn<sub>17</sub> cluster 5 can be described as two merged Sn<sub>9</sub> subunits, which already shows that larger clusters might be seen as cluster of clusters, where we will see more examples in the following. Anionic Sn<sub>9</sub> clusters are also known from Zintl-Ion chemistry, where the structures often nicely fit Wades rules<sup>22,23</sup> and which are summarized in recent reviews.<sup>24,25</sup> However, Zintl-Ions will not be included in the following as the focus of the perspective is on metalloid clusters, exhibiting an average positive oxidation state of the tin atoms in contrast to Zintl-Ions exhibiting an average negative oxidation state.<sup>26</sup>

## Synthesis *via* disproportionation reaction

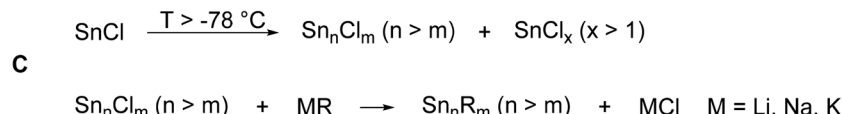
Beside reductive coupling, another approach to metalloid clusters can be seen in the disproportionation reaction of useful precursors. The disproportionation reaction should take place at low temperatures so that the intermediary formed metalloid

clusters can be trapped by kinetic stabilization. In case of tin, metastable monohalide solutions, obtained *via* a preparative co-condensation technique, seem feasible,<sup>27,28</sup> following the reaction scheme outlined in Scheme 2.

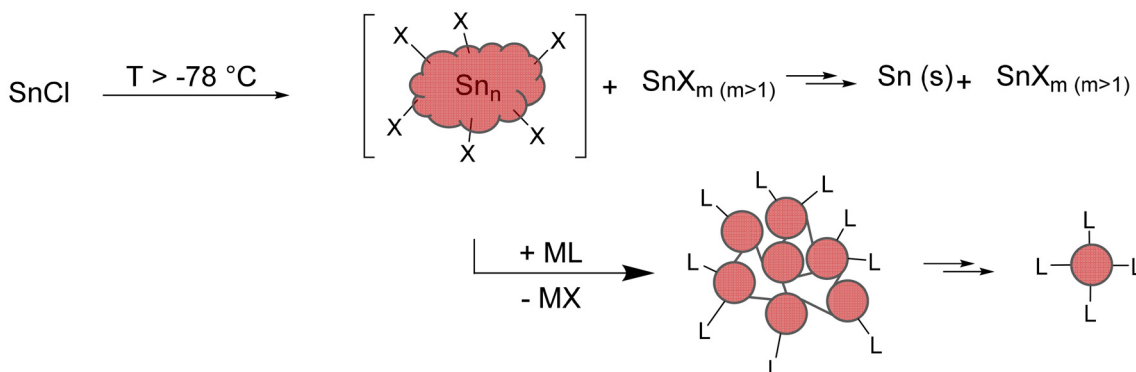
Hence, the isolated clusters are not only intermediates on the way to the element with respect to the average oxidation state of the tin atoms, but also with respect to the synthetic route as without the substitution of the halide atoms by bulky ligands, the disproportionation reaction directly gives elemental tin (Scheme 3).

Additionally, calculations indicate that in the size range up to 309 tin atoms, structures that can be described as cluster of clusters are energetically favourable, which leads to the general reaction scheme outlined in Scheme 3. Hence, the intermediary formed clusters can be seen as a cluster-of-clusters arrangement, where the principal units are bound together by tin-tin bonds. These primary formed clusters then might be stable and can be isolated, or they can fall apart, leading to smaller clusters with an open substituent shell. Consequently, the bonding between the principal units in the larger clusters is of central importance if larger or smaller metalloid clusters are obtained.

This general idea (raspberry model) about the formation mechanism is supported by the reaction of a metastable Sn(*i*)



**Scheme 2** Formation of tin clusters *via* the disproportionation reaction (C).



**Scheme 3** Schematic visualization of the raspberry model. Formation of smallest  $\text{Sn}_{10}$ -units (e.g.,  $[\text{Sn}_{10}(\text{Hyp})_4]^{2-}$ ) through the degradation of larger clusters.

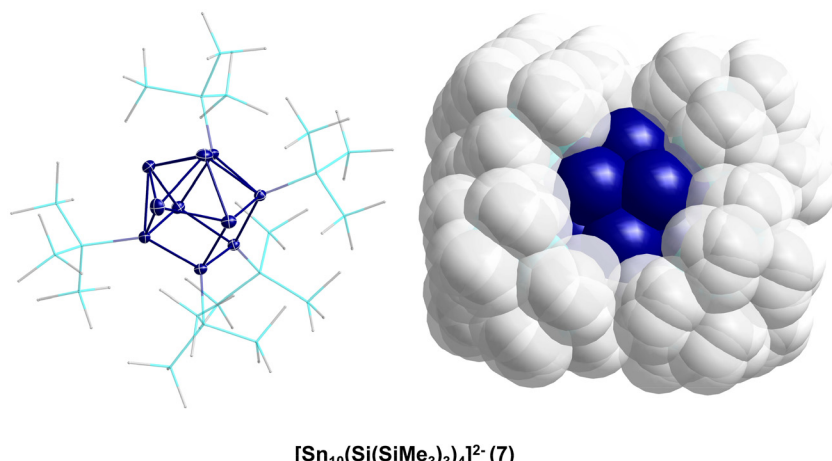


**Fig. 2** Left: molecular structure of  $[\text{Sn}_{10}(\text{Hyp})_4]^{2-}$  (7). The Hyp-substituents are simplified by wires and sticks, and hydrogen atoms are omitted for clarity (light blue = silicon, grey = carbon, and dark blue = tin). Right: space-filling model of 7 with the open ligand shell visible.

Cl solution with LiHyp (Hyp =  $\text{Si}(\text{SiMe}_3)_3$ ), which gives after work-up the metalloid tin cluster  $[\text{Sn}_{10}(\text{Hyp})_4]^{2-}$  7 (Fig. 2)<sup>29</sup> in remarkable 33% isolated crystalline yield.

Thereby, the substituent shell is quite open as the four Hyp substituents shield the core of ten tin atoms only marginally (Fig. 2, right). In solution, 7 is stable for a couple of days if  $\text{Li}^+$  is coordinated by (12)-crown-4. However, if 7 is transferred to the gas-phase *via* electrospray ionization,  $[\text{Hyp}]^-$  or  $[\text{SnHyp}]^-$  is eliminated, leading to  $[\text{Sn}_{10}(\text{Hyp})_3]^-$  8<sup>30</sup> or  $[\text{Sn}_9(\text{Hyp})_3]^{2-}$  9, respectively. Both compounds are also obtained directly applying the disproportionation reaction, indicating that a complex reaction mixture is obtained first, from which, depending on the work-up of the reaction solution, different metalloid clusters are obtained (Fig. 3). Beside the already mentioned clusters, the following clusters are available:  $[\text{Sn}_9(\text{Hyp})_3]^-$  10,<sup>31</sup>  $[\text{Sn}_9(\text{Hyp})_2]^{2-}$  11,<sup>32</sup>  $[\text{Sn}_{10}(\text{Si}(\text{SiMe}_3)_2(\text{Si}(\text{SiMe}_3)_3)_4)]^{2-}$  12,<sup>33</sup>  $[\text{Sn}_{10}(\text{Si}(\text{SiMe}_3)_2(\text{Si}^t\text{BuMe}_2))_4]^{2-}$  13,<sup>34</sup>  $[\text{Sn}_{10}(\text{Ge}(\text{SiMe}_3)_4)]^{2-}$  14,<sup>35</sup>  $[\text{Sn}_{10}(\text{R})_5]^-$  (R = Hyp 15,<sup>36</sup> Ge(SiMe<sub>3</sub>)<sub>3</sub> 16<sup>35</sup>), and  $\text{Sn}_{10}(\text{R})_6$  (R = Hyp 17,<sup>37</sup> Ge(SiMe<sub>3</sub>)<sub>3</sub> 18<sup>35</sup>).

Within all the metalloid tin clusters exhibiting 10 tin atoms (7, 8, 12–18) the arrangement of tin atoms can be described as

a more or less distorted centaur polyhedral arrangement, where the tin–tin distances within the icosahedral part are longer and comparable to the distances found in  $\beta$ -tin. The distances in the cubic part are shorter and comparable to the distance found in  $\alpha$ -tin. These different kinds of tin atoms are also observed within the Mößbauer spectra, supporting the idea that a phase transition takes place on going from the cubic to the icosahedral part of the cluster. In case of 17, the tin core is well shielded by the six Hyp substituents so that further reactions might not be possible. However, in case of clusters 7–16, the nine or ten tin atoms are only partially shielded by the bulky substituents so that subsequent reactions might be possible.

Such subsequent reactions are well documented for the metalloid germanium clusters  $[\text{Ge}_9(\text{Hyp})_3]^-$  (ref. 38 and 39) and  $[\text{Ge}_9(\text{Hyp})_2]^{2-}$ ,<sup>40</sup> where oxidative coupling was also realized to give neutral clusters of the composition  $[\text{Ge}_{18}(\text{Hyp})_6]$ .<sup>41,42</sup>

That such subsequent reactions of open shell metalloid tin clusters are also possible was shown in 2017 for  $[\text{Sn}_{10}(\text{Hyp})_4]^{2-}$  7. Thereby, the reaction of 7 with  $(\text{Ph}_3\text{P})\text{Au}(\text{i})\text{SHyp}$  gives the cluster compound  $[\text{Au}_3\text{Sn}_{18}(\text{Hyp})_8]^-$  19.<sup>43</sup> Within 19, two



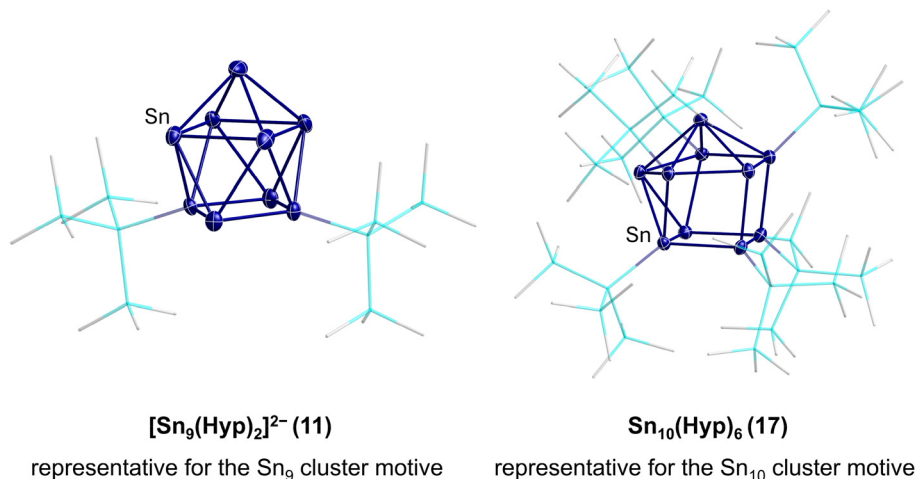


**Fig. 3** Examples for metalloid clusters synthesized via the disproportionation reaction. Ligands are simplified by wires and sticks, hydrogen atoms are omitted for clarity (light blue = silicon, light grey = carbon, and dark blue = tin).

Sn<sub>9</sub>(Hyp)<sub>3</sub> units are bound together by a central Au atom and capped on the other side with an Au(Hyp) unit (Fig. 4).

This result directly shows that with respect to germanium, in the case of tin, a more complex reaction system is present as not only can a coordination or a salt metathesis reaction take place but the cluster itself can also decompose, leading to Sn<sub>9</sub>(Hyp)<sub>3</sub> units in this case. Another strong difference with the chemistry of the open shell metalloid germanium clusters is the fact that product **19** is also quite sensitive and decomposes fast in solution to unknown products. In contrast to this, the structurally comparable compound PtZn<sub>2</sub>Ge<sub>18</sub>(Hyp)<sub>8</sub> is stable in solution.<sup>44</sup> The higher sensitivity and dynamic of the metalloid tin clusters with respect to the metalloid germanium clusters might be due to the weaker tin–tin bonds with respect to germanium–germanium bonds. The higher metallic character of tin may also be another factor so that in case of tin, higher coordination

numbers are easily realized. To date, mostly hypersilyl-based substituents are used for the synthesis. However, it is known in cluster chemistry that the substituent applied also has an influence on the reactivity and stability of the obtained compound. Consequently, also other substituents were used within the synthesis *via* the disproportionation reaction, for example, the sterically more demanding substituent Si*t*Bu<sub>3</sub>, leading to Sn<sub>20</sub>(Si*t*Bu<sub>3</sub>)<sub>10</sub>Cl<sub>2</sub> **20**, where not all the halide atoms are substituted and which shows a unique arrangement of the tin atoms, further supporting the raspberry model discussed above.<sup>45</sup>

## Cluster of clusters

The Sn<sub>17</sub> cluster **5**, synthesized by Fischer *et al.*, might already be described as a cluster built up of two principal Sn<sub>9</sub> clusters fused together by one tin atom, belonging to both Sn<sub>9</sub> units. The Sn<sub>9</sub> framework is thereby well known from metalloid tin clusters or from various Zintl-phases<sup>24,25,46</sup> and can therefore be considered as the “smallest” tin-unit in **5**. Consequently, the structure of **5** directly provides evidence that larger clusters might be composed of smaller units, as described in the cluster-of-clusters model. While the use of the bulky Si(SiMe<sub>3</sub>)<sub>3</sub> substituents within the synthetic route *via* the disproportionation reaction almost exclusively leads to Sn<sub>10</sub> or Sn<sub>9</sub> clusters, the use of the bulky ligand Si*t*Bu<sub>3</sub> leads to a different compound. Hence, this time, another Sn<sub>9</sub> or Sn<sub>10</sub> cluster with an open substituent shell is not realized but the metalloid cluster Sn<sub>20</sub>(Si*t*Bu<sub>3</sub>)<sub>10</sub>Cl<sub>2</sub> **20** with 20 tin atoms is obtained. **20** is the largest structurally characterized metalloid group 14 cluster and is obtained *via* the disproportionation route using an SnCl solution and NaSi*t*Bu<sub>3</sub> as the substituent source.<sup>45</sup>

The structure of **20** is remarkable as it can be divided into three subunits (Fig. 5). In the centre, there is an Sn<sub>8</sub> unit of naked tin atoms, which exhibits a distorted cubic arrangement (purple polyhedra, Fig. 5). The cubic arrangement thereby resembles the

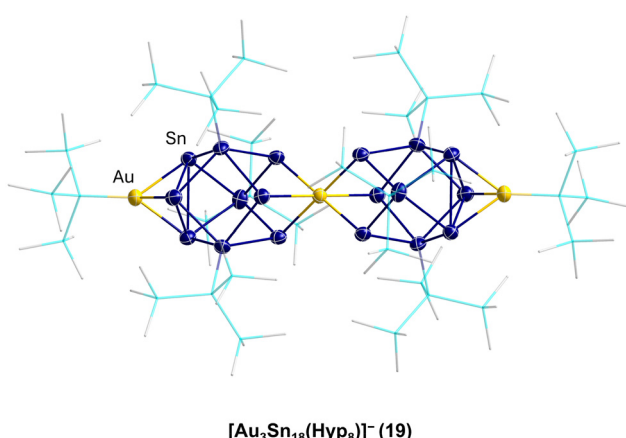


**Fig. 4** First use of the [Sn<sub>9</sub>Hyp<sub>3</sub>]<sup>-</sup> cage as a ligand in coordination chemistry to form **19**. Ligands are simplified by wires and sticks, and hydrogen atoms are omitted for clarity (light blue = silicon, light grey = carbon, yellow = gold, and dark blue = tin).



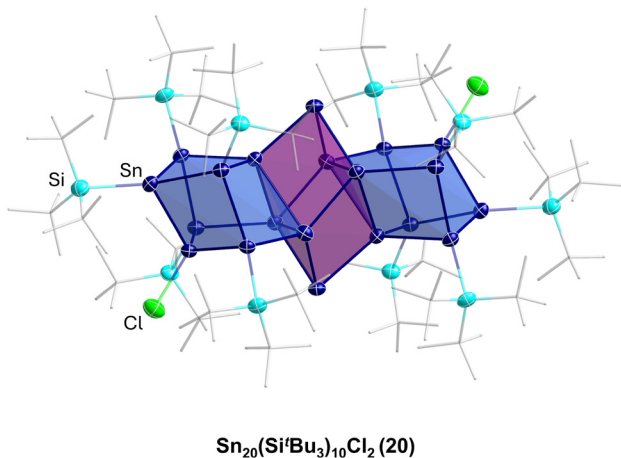
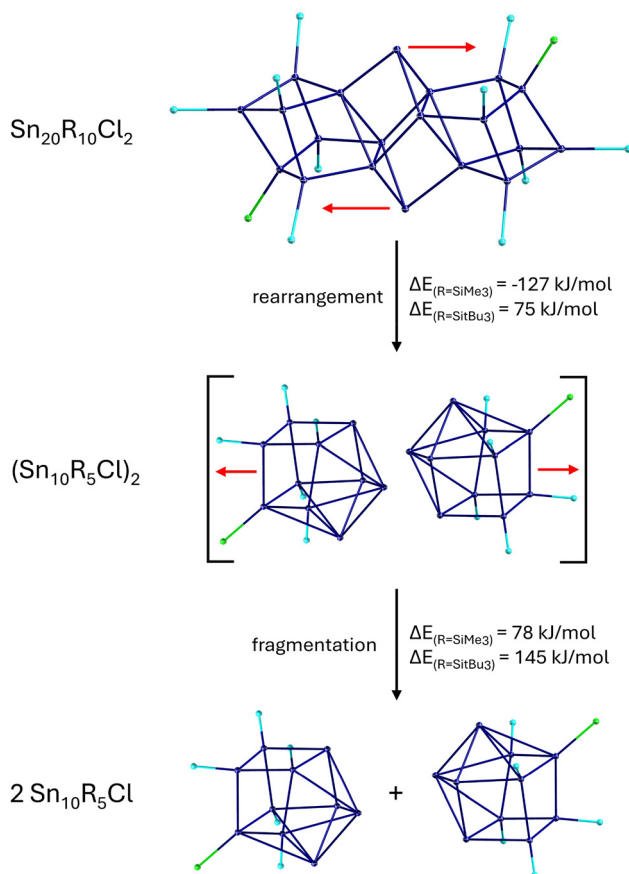


**Fig. 5** Molecular structure of  $\text{Sn}_{20}(\text{Si}^t\text{Bu}_3)_{10}\text{Cl}_2$  (**20**). The  $\text{Si}^t\text{Bu}_3$ -substituents are simplified by wires and sticks, hydrogen atoms are omitted for clarity (light blue = silicon, green = chloride, dark blue = tin).



**Scheme 4** Possible decomposition pathway of **20** via rearrangement and fragmentation. Energies calculated for two substituents ( $R = \text{SiMe}_3$ ,  $\text{Si}^t\text{Bu}_3$ ).

one found in the metalloid cluster  $\text{Sn}_8\text{R}_4$  ( $R = 2,6\text{-Mes}_2\text{C}_6\text{H}_3$ ; Mes = 2,4,6-Me<sub>3</sub>C<sub>6</sub>H<sub>2</sub>)<sup>15</sup> with comparable tin-tin distances. To this central  $\text{Sn}_8$  unit, two  $\text{Sn}_6\text{R}_5\text{Cl}$  units are bound *via* tin-tin

single bonds in the range of 282.3(2)–288.20(19) pm (blue polyhedra, Fig. 5). Within the  $\text{Sn}_6\text{R}_5\text{Cl}$  unit, every tin atom bears a substituent and exhibits the coordination number four, leading to a classical bonding as within the prismatic clusters  $\text{Sn}_6\text{R}_6$  ( $R = \text{Si}^t\text{Bu}_3$ ).<sup>47</sup> The  $\text{Sn}_{20}$  cluster **20** thus strongly supports the aspect that cluster growth in the nanometre range takes place *via* cluster of clusters intermediates and depending on the substituent, they might be isolated or decomposed to smaller principal units.

This idea is further supported by calculations focussing on the decomposition of **20** into two  $\text{Sn}_{10}$  clusters as these are the ones frequently obtained when  $\text{Si}(\text{SiMe}_3)_3$  is used as the ligand source. The structural relation of **20** and a metalloid  $\text{Sn}_{10}$  cluster becomes obvious on moving the central tin atoms, as outlined in Scheme 4.

After this movement, two loosely bound  $\text{Sn}_{10}\text{R}_5\text{Cl}$  clusters are realized, which then might dissociate to give smaller less shielded clusters. The movement of the two tin atoms is endothermic in case of the used  $\text{Si}^t\text{Bu}_3$  substituent. However, if the much smaller  $\text{SiMe}_3$  substituent is used for the calculations, the movement of the tin atoms becomes exothermic, directly showing that the substituent applied has a strong influence if the cluster-of-clusters arrangement or the decomposition to smaller principal units is energetically more favourable. Consequently, to get access to larger metalloid clusters, the choice of the substituent is of central importance.

## Conclusion and future outlook

Metalloid tin clusters are ideal atomically precise model compounds for the nanoscaled area, showing novel structures and bonding properties. The naked tin atoms are ideal positions for further reactions, which may also be reversible ones for catalytic applications. However, the subsequent reactions lead up to now always to a decomposition of the primary products. In the area of larger clusters, a cluster of clusters growth seems obvious and thus to get stable larger metalloid tin clusters, useful substituents are needed. Multidentate substituents might be useful to stabilize the intermediary formed larger clusters as these substituents might be able to stabilize the cluster-of-clusters state so that further insight into the fascinating process of cluster growth on the way to the element is possible. However, if the cluster size increases more, the transition area from the cluster of clusters to compact structures would be another interesting area, which might be reached a bit earlier in the case of substituent-stabilized clusters than the naked cluster used during the calculations. The route *via* disproportionation seems to be the most useful as it intrinsically leads to elemental tin, but we need to find the right reaction conditions and substituents to stop this route in the nanometre range.

## Author contributions

Roman Kimmich – conceptualization, visualization, writing – original draft, and writing – review and editing. Andreas



Schnepf – conceptualization, funding acquisition, project administration, validation, resources, supervision, and writing – review and editing.

## Data availability

No primary research results, software or code has been included and no new data were generated or analysed as part of this review.

## Conflicts of interest

There are no conflicts to declare.

## Acknowledgements

The authors thank Dr Claudio Schrenk for helpful discussions and the German Research Foundation (DFG) for financial support through grant no. SCHA738/12-1.

## References

- 1 L. R. Sita and R. D. Bickerstaff, *J. Am. Chem. Soc.*, 1989, **111**, 6454–6456.
- 2 L. R. Sita and I. Kinoshita, *J. Am. Chem. Soc.*, 1992, **114**, 7024–7029.
- 3 Structurally related compounds like bicyclo[2.2.1]heptastannane-1,4-diide and bicyclo[2.2.2]octastannane-1,4-diide have been lately presented by Liptrop and Fischer, (*Chem. Commun.*, 2020, **56**, 336).
- 4 L. R. Sita, *Acc. Chem. Res.*, 1994, **27**, 191–197.
- 5 L. R. Sita and R. D. Bickerstaff, *J. Am. Chem. Soc.*, 1989, **111**, 3769–3770.
- 6 L. R. Sita and I. Kinoshita, *Organometallics*, 1990, **9**, 2865–2867.
- 7 A. Schnepf and H. Schnöckel, *Angew. Chem., Int. Ed.*, 2002, **41**, 3532–3554.
- 8 A. Lechtken, N. Drebov, R. Ahlrichs, M. M. Kappes and D. Schooss, *J. Chem. Phys.*, 2010, **132**, 211102.
- 9 H. Li, W. Chen, F. Wang, Q. Sun, Z. X. Guo and Y. Jia, *Phys. Chem. Chem. Phys.*, 2013, **15**, 1831–1836.
- 10 Results of a PhD-thesis (C. Zeppek, 2015) and a master thesis (S. Reischauer, 2018) prepared in the Uhlig group at TU Graz.
- 11 N. Wiberg, H.-W. Lerner, S. Wagner, H. Nöth and T. Seifert, *Z. Naturforsch., B: J. Chem. Sci.*, 1999, **54**, 877–880.
- 12 R. Bashkurov, Y. Kratish, N. Fridman, D. Bravo-Zhivotovskii and Y. Apeloig, *Angew. Chem., Int. Ed.*, 2021, **60**, 2898–2902.
- 13 A. Schnepf and R. Köppe, *Angew. Chem., Int. Ed.*, 2003, **42**, 911–913.
- 14 A. Schnepf and C. Drost, *Dalton Trans.*, 2005, 3277–3280.
- 15 B. E. Eichler and P. P. Power, *Angew. Chem., Int. Ed.*, 2001, **40**, 796–797.
- 16 N. Y. Tashkandi, E. E. Cook, J. L. Bourque and K. M. Baines, *Chem. – Eur. J.*, 2016, **22**, 14006–14012.
- 17 J. Wiederkehr, C. Wölper and S. Schulz, *Chem. Commun.*, 2016, **52**, 12282–12285.
- 18 M. Brynda, R. Herber, P. B. Hitchcock, M. F. Lappert, I. Nowik, P. P. Power, A. V. Protchenko, A. Růžička and J. Steiner, *Angew. Chem., Int. Ed.*, 2006, **45**, 4333–4337.
- 19 A. Rodig and G. Linti, *Angew. Chem., Int. Ed.*, 2000, **39**, 2952–2954.
- 20 C. Schenk, F. Henke and A. Schnepf, *Angew. Chem., Int. Ed.*, 2013, **52**, 1834–1838.
- 21 G. Prabusankar, A. Kempter, C. Gemel, M. K. Schröter and R. A. Fischer, *Angew. Chem., Int. Ed.*, 2008, **47**, 7234–7237.
- 22 K. Wade, *J. Chem. Soc. D*, 1971, **15**, 792–793.
- 23 D. M. P. Mingos, *Nat. Phys.*, 1972, **236**, 99–102.
- 24 S. Scharfe, F. Kraus, S. Stegmaier, A. Schier and T. F. Fässler, *Angew. Chem., Int. Ed.*, 2011, **50**, 3630–3670.
- 25 R. J. Wilson, B. Weinert and S. Dehnen, *Dalton Trans.*, 2018, **47**, 14861–14869.
- 26 A. Schnepf, in *Clusters – Contemporary Insight in Structure and Bonding*, ed. S. Dehnen, Springer International Publishing, Chem, 2017, pp. 135–200.
- 27 C. Schrenk, R. Köppe, I. Schellenberg, R. Pöttgen and A. Schnepf, *Z. Anorg. Allg. Chem.*, 2009, **635**, 1541–1548.
- 28 M. Binder, C. Schrenk and A. Schnepf, *J. Visualized Exp.*, 2016, **117**, e54498.
- 29 C. Schrenk, F. Winter, R. Pöttgen and A. Schnepf, *Chem. – Eur. J.*, 2015, **21**, 2992–2997.
- 30 C. Schrenk, B. Gerke, R. Pöttgen, A. Clayborne and A. Schnepf, *Chem. – Eur. J.*, 2015, **21**, 8222–8228.
- 31 C. Schrenk, M. Neumaier and A. Schnepf, *Inorg. Chem.*, 2012, **51**, 3989–3995.
- 32 C. Schrenk, F. Winter, R. Pöttgen and A. Schnepf, *Inorg. Chem.*, 2012, **51**, 8583–8588.
- 33 C. Schrenk and A. Schnepf, *Main Group Met. Chem.*, 2013, **36**, 161–167.
- 34 R. Kimmich, C. Schrenk and A. Schnepf, *Dalton Trans.*, 2021, **50**, 16013–16020.
- 35 M. Binder, C. Schrenk, T. Block, R. Pöttgen and A. Schnepf, *Molecules*, 2018, **23**, 1022.
- 36 C. Schrenk, J. Helmlinger and A. Schnepf, *Z. Anorg. Allg. Chem.*, 2012, **638**, 589–593.
- 37 C. Schrenk, I. Schellenberg, R. Pöttgen and A. Schnepf, *Dalton Trans.*, 2010, **39**, 1872–1876.
- 38 F. Henke, C. Schenk and A. Schnepf, *Dalton Trans.*, 2009, 9141–9145.
- 39 C. Schenk and A. Schnepf, *Angew. Chem., Int. Ed.*, 2007, **46**, 5314–5316.
- 40 F. S. Geitner and T. F. Fässler, *Inorg. Chem.*, 2020, **59**, 15218–15227.
- 41 O. Kysliak, C. Schrenk and A. Schnepf, *Angew. Chem., Int. Ed.*, 2016, **55**, 3216–3219.
- 42 S. V. Klementyeva, C. Schrenk and A. Schnepf, *Inorg. Chem.*, 2022, **61**, 11787–11795.



43 M. Binder, C. Schrenk, T. Block, R. Pöttgen and A. Schnepf, *Chem. Commun.*, 2017, **53**, 11314–11317.

44 O. Kysliak, D. D. Nguyen, A. Z. Clayborne and A. Schnepf, *Inorg. Chem.*, 2018, **57**, 12603–12609.

45 M. Binder, C. Schrenk and A. Schnepf, *Chem. Commun.*, 2019, **55**, 12148–12151.

46 H. G. Von Schnerring, M. Baitinger, U. Bolle, W. Carrillo-Cabrera, J. Curda, Y. Grin, F. Heinemann, J. Llanos, K. Peters, A. Schmeding and M. Somer, *Z. Anorg. Allg. Chem.*, 1997, **623**, 1037–1039.

47 N. Wiberg, H. W. Lerner, H. Nöth and W. Ponikwar, *Angew. Chem., Int. Ed.*, 1999, **38**, 1103–1105.

